The Elastodynamics of Embryonic Epidermal Wound Closure

By Alexander Sadovsky and Frederic Y. M. Wan

This paper is concerned with the elastodynamics of embryonic epidermal wound closing. Underlying the recovery process for this type of wounds is a mechanism of wound recognition through directed cell-to-cell signaling. The observed actin filament realignment induced by the biological signals leads to a purse-string effect and the resulting (unknown) "active stresses." The circumferential contraction of the epidermis surrounding the wound is then determined by the laws of mechanics and propagation properties of the relevant cell–cell signaling that decays with distance. With the wound known to retract for a short period immediately after infliction, the quasi-equilibrium configuration reached during this initial phase serves as the initial condition for the dynamic wound closing phase. A small strain variation of the Murray–Sherratt model of the quasi-equilibrium problem will be formulated for speedy computation of this initial state at the inception of the wound closure phase, with the latter problem being the main concern of this paper. Some theoretical developments are found to be instrumental to an efficient algorithm for the otherwise time-consuming task of calculating the effect of the biological signals generated by the presence of a wound. Application of our elastodynamic model to the case of a circular wound suggests that the propagation range of our choice of cell–cell signaling mechanism must be above a certain minimum fraction of the wound radius for wound closure. As expected, stress concentration occurs adjacent to the edge of the remaining small wound near the end of the wound

Address for correspondence: Frederic Y. M. Wan, Department of Mathematics, University of California, Irvine, Irvine, CA 92697-3875; e-mail: fwan@math.uci.edu

STUDIES IN APPLIED MATHEMATICS 118:365–395

Published by Blackwell Publishing, 350 Main Street, Malden, MA 02148, USA, and 9600 Garsington Road, Oxford, OX4 2DQ, UK.

closing process. At that point, the present model is not expected to be adequate and more appropriate expressions of elastic strain and active stress induced by actin filaments may be in order. Other biological processes such as cell proliferation and differentiation may be involved.

1. Introduction

This paper is concerned with the elastodynamics of *epidermal wound closure* in *embryonic* mammalian skin. Interest in wound healing probably existed long before recorded history and the medical literature on this subject is vast (see [1, 2] for some pertinent references). Nevertheless, the underlying bio-dynamical process of wound healing is still far from well understood. It is customary to divide wound healing into three stages, inflammation, wound closure, and extracellular matrix remodeling in scar tissue, though the boundaries of the stages are not sharp. Even if we focus on the wound closure stage, as we will do here, it is still necessary to distinguish the closure process in *dermal* (i.e., full-depth skin) wounds from that in wounds no deeper than the outermost layer of skin, that is, injuries to the *epidermis*. In dermal wounds, the wound opening is closed by epidermal cell migration and granulation tissue contraction [3]. These processes have been studied relatively extensively (see chapter 10 of [2]). The closure of epidermal wounds is better understood for *adult* skin. For such wounds, it is generally accepted that re-epithelialization is due entirely to epidermal cells at the wound edge moving inwards to close the wound. For *embryonic* epidermal wound closure, there is much less agreement except that it is quite different from the aforementioned re-epithelialization of adult epidermal wounds [4] and that embryonic wounds heal without scarring. In this paper, we focus on this less well understood type of wound healing, often without explicitly stating the embryonic and epidermal nature of the wound.

Experimental evidence [5, 6] (see also [3]) suggests that a *circumferential tension* at the wound edge may well be the mechanism underlying embryonic epidermal movement, acting like a purse string that pulls the wound edge inwards. The work of Martin and Lewis [5, 6] revealed a thick cable of actin around the epidermal wound margin localized within the leading row of basal cells. The review article [3] indicated that immediately after wound infliction, the edge of the wound begins to retract (see Figure 1). Concurrently, the actin filaments in the wound margin realign and an actin cable is formed within a few minutes (see cartoon in Figure 2). The retraction stops as the epidermis reaches a post-wounding quasi-equilibrium. The cable generally takes up to an hour or more to attain its full thickness and persists thereafter. Shortly after the wound edge reaching quasi-equilibrium, the tension in the cable begins

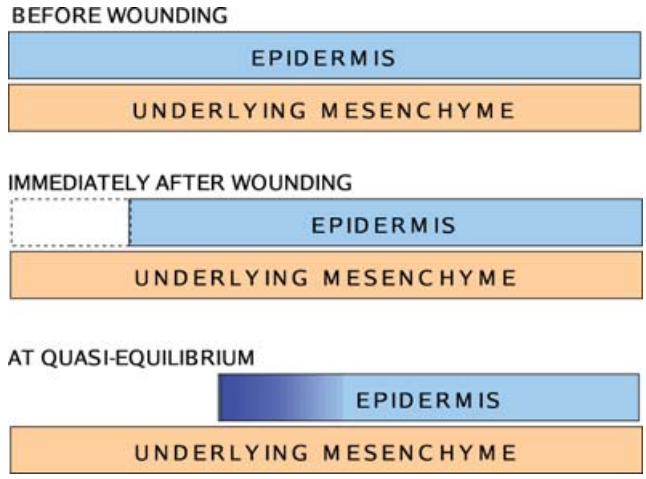

Figure 1. Basic skin layers and the post-wounding epidermal retraction. The quasi-equilibrium (bottom) is achieved through the formation of an actin cable, depicted in Figure 2.

to drive the cable to act like a purse string that contracts inward, causing epidermal migration, and eventual wound closure.

The observations in [5, 6, 3] led Murray and his collaborators to formulate appropriate mechanical models to characterize the quasi-equilibrium state of the deformable wound at the end of the epithelial retraction. All these models

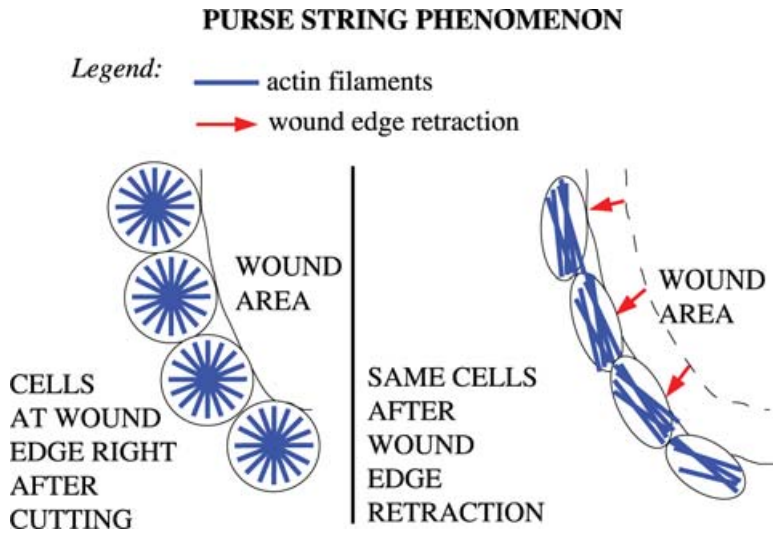

Figure 2. The actin cable formation leading to a post-wounding quasi-equilibrium. *Left:* Immediately after the wound is inflicted, the epidermis has not retracted, and the shown actin filaments have no preferred orientation. *Right:* The epidermis has retracted, and the actin filaments realign along a preferred direction to form a cable. Subsequently, the cable acts as a contracting purse string.

are modifications of an earlier mechanochemical model by Murray and Oster for the deformation of the epithelial sheet [7, 8]. The results from the analyses of these models have provided a good understanding of this initial retraction phase of the embryonic epidermal wound healing process.

With the experimental evidence of (intracellular) actin filaments re-aligning (and linked by cell–cell adherens junctions) into an actin cable at the wound edge, there is some agreement that the subsequent contraction phase of embryonic epidermal wound closure is due to a purse string effect associated with the tightening of the actin cable. However, there is still no general agreement on how the cable causes the wound to contract. Central to the problem is the question of how cells surrounding the wound sense the presence of the wound and then react by further tightening the actin cable. The present work offers a possible mechanism for the embryonic epidermal wound closing process by the adoption of a plausible wound sensing and local response protocol. The elastodynamics of the epidermis is then expected to drive the edge of the wound to contract toward closure. Implicit in this mechanical model of wound closure is an assumption that chemotaxis, the phenomenon of cells traveling in response to a chemical signal, does not have a substantive role in embryonic wound healing during the wound closure phase. Some justification will be provided for this position when we formulate our cell–cell signaling protocol in Section 3.

The contraction phase of wound healing begins shortly after the wound edge reaches a state of quasi-static equilibrium. We will start with the particular model developed in [2], called the Murray–Sherratt model henceforth, and use a small strain variation of that model to provide the initial conditions for the elastodynamical model developed herein for the contraction phase. Quasi-equilibrium states of the wound determined by these models have been obtained for circular wounds as well as for elliptical wounds in [9]. The circular wound case has been previously treated by Sherratt using several variants of the Murray–Sherratt finite strain model [10, 11] (see also [2]). The investigation of elliptical wounds in [9], however, was the first treatment of a noncircular wound shape for embryonic wounds. Both will serve as the initial states for the dynamic evolution of wound closure, which is the main concern of this paper. The efficacy of our dynamic model for the contracting phase of wound healing will be established and illustrated by the circular wound case in this paper. Results for the more complicated case of elliptical wounds will be reported in a separate publication [12].

For computational expediency, we will work a small strain version of the Murray–Sherratt model which offers significant computational advantages by reducing the extensive numerical simulations in testing the elastodynamical model for wound contraction. This simplification is not a limitation to the proposed wound closing model since the same cell signal sensing mechanism applies to a suitable elastomechanical description of any quasi-static equilibrium phase of the wound.

We focus on embryonic epidermal wounds in part because there has been much less analytical investigation (compared to adult epidermal wounds and dermal wounds) to gain insight to the healing process for this class of wounds. In fact, there has been no elastodynamic modeling and analysis of the wound closing process following quasi-equilibrium for such wounds. Our study of the elastodynamics of wound closure has the advantage that it may be undertaken independently of the other wound recovery phenomena, for example, inflammation, dermal migration, extracellular matrix re-configuration in scar tissue, etc., keeping in mind that embryonic epidermal wounds heal without scarring. There is not a great deal of experimental data on embryonic epidermal wounds in the wound literature. We hope that the results of our analytical investigation would stimulate suitable experimental work in this field; our effort certainly has uncovered areas where quantitative information on wound sensing and constitutive relations are lacking and very much needed for theoretical studies of the embryonic epidermal wound healing phenomenon.

2. The quasi-static equilibrium phase

2.1. The Murray–Sherratt model

It is known that immediately after infliction, an epidermal wound edge retracts; concurrently actin filaments realign in the wound margin. After the actin purse-string has been formed, the retraction stops, and the epidermis assumes a state of post-wounding quasi-equilibrium for some duration before the wound begins to close. The sequence of events is shown in Figure 1. The quasi-equilibrium configuration reached during the initial retraction phase will therefore be needed as the initial condition for the dynamic wound closing phase, which is the main interest of this paper. We will summarize in this section the quasi-equilibrium model for epidermal wounds described in [2] to be used in our dynamic wound closing model whenever it is needed.

As in previous treatments of epidermal wounds, the wounded epidermis is regarded as a two-dimensional homogeneous, isotropic, elastic (epithelial) sheet surrounding a simply connected wound with edge curve Σ. With the sheet (temporarily) in a state of elastostatic equilibrium, the two-dimensional stress tensor $\boldsymbol{\sigma}$ that characterizes the internal force field of the sheet is related to the restoring force intensity vector $\vec{f}$ by the vector partial differential equation of force balance,

$$\vec{\nabla} \cdot \boldsymbol{\sigma} = \vec{f}, \tag{1}$$

in the region Ω exterior to the simple smooth (wound edge) curve Σ. (For the sample solutions computed in this paper, Σ will be a circle. The more general case of elliptical wounds, also treated in [9], will be reported in a

future publication [12].) In the Murray–Sherratt model, the stress tensor $\boldsymbol{\sigma}$ is given in terms of the displacement vector field $\vec{u}$ defined in the elastic sheet domain Ω by the constitutive relation

$$\begin{aligned}\boldsymbol{\sigma} &= \text{elastic stresses} + \text{active contraction stress} \\ &= G[E\boldsymbol{\epsilon} + \Gamma(\vec{\nabla}\cdot\vec{u})\mathbf{I}] + \tau G\mathbf{I}. \end{aligned} \tag{2}$$

In Equation (2), $\boldsymbol{\epsilon}$ is the strain tensor of the elastic sheet, $\frac{1}{2}E$ and Γ are the Lamé constants (more conventionally designated as μ and λ, respectively), $G(\vec{x})$ is the density of the intracellular actin filaments at the material point initially at the position $\vec{x} = (x_1, x_2)$, and the traction τ in the active contraction stress term is taken to be

$$\tau = \frac{\tau_0}{1-\beta\Delta} \simeq \frac{\tau_0}{1+\beta\vec{\nabla}\cdot\vec{u}}, \tag{3}$$

where Δ is the actin filament (extension or) compaction, taken to a first approximation to be $-\vec{\nabla}\cdot\vec{u}$ (as long as $0 > \vec{\nabla}\cdot\vec{u} \gg -1$). In (3), β is a constant quantifying the effect of compacting the actin filaments (see [2]) and the parameter τ_0 is the sum of the two constant principal stresses in the absence of actin filament compaction. Consistent with the notation of [2], E, normally denoting Young's modulus in engineering literature, here denotes twice the shear modulus of the elastic sheet [13].

In the Murray–Sherratt model, the elastic strain tensor $\boldsymbol{\epsilon}$ is given in terms of $\vec{u}$ by the linear strain-displacement relations below in tensor/dyadic notations:

$$\boldsymbol{\epsilon} = \frac{1}{2}\big(\vec{\nabla}\vec{u} + (\vec{\nabla}\vec{u})^T\big). \tag{4}$$

The restoring force intensity $\vec{f}$ due to the underlying substratum below the skin via cellular attachments [14] is modeled by a spring force $\lambda G\vec{u}$, where λ is a parameter quantifying the strength of the restoring force exerted by the mesenchyme underlying the epidermis.

The actin filament density G is related to the amount of compaction Δ of the tissue resulting from the displacements $\vec{u}$ of the neighboring points from their initial positions. It is assumed that the amount of filamentous actin remains constant in a given region of the unwounded part of the epidermis while it deforms as a consequence of the wound injury [1]. This implies that the actin density function G satisfies the conservation law $G(\vec{x})(1-\Delta) = \kappa$ for some constant κ. With $\Delta \simeq -\vec{\nabla}\cdot\vec{u}$, we have

$$G(\vec{x})(1+\vec{\nabla}\cdot\vec{u}) = \kappa. \tag{5}$$

With (2)–(5), the local equilibrium condition (1) may be written as

$$\vec{\nabla}\cdot\left[\frac{1}{1+\vec{\nabla}\cdot\vec{u}}\left(E\boldsymbol{\epsilon} + \Gamma\vec{\nabla}\cdot\vec{u}\mathbf{I} + \frac{1}{1+\beta\vec{\nabla}\cdot\vec{u}}\mathbf{I}\right)\right] - \frac{\lambda\vec{u}}{1+\vec{\nabla}\cdot\vec{u}} = \vec{0}. \tag{6}$$

Note that the constant κ has no role in the final form of the equation of local equilibrium since it is a common factor for all terms of the equation (given that $G(\vec{x})$ is a common factor for all terms in $\boldsymbol{\sigma}$). We have also set $\tau_0 = 1$ so that the parameters E, Γ and λ are in unit of τ_0 (and numerically equal to E/τ_0, Γ/τ_0, and λ/τ_0). This leaves β as the only parameter of the problem in addition to the scaled elastic moduli E, Γ, and λ. We will say more about these four scaled parameters in the next section.

The vector partial differential equation (6) is supplemented by the stress-free boundary condition along the wound edge,

$$\boldsymbol{\sigma} \cdot \vec{n} = \vec{\sigma}_n = \vec{0} \quad \text{along } \Sigma, \tag{7}$$

where $\vec{n}$ is the unit outward normal vector of the edge curve Σ, and the quiescent condition far away from the wound in all directions:

$$\vec{u} \to \vec{0} \quad \text{as } |\vec{x}| \to \infty. \tag{8}$$

It should be evident from the relevant equations that the Murray–Sherratt formulation of the quasi-static equilibrium configuration of epidermal wound is frame-invariant.

For a circular wound of radius a (typically of the order of 500 microns), a polarly (rotationally) symmetric quasi-equilibrium state may be obtained by specializing the boundary value problem (BVP) (6)–(8) to polar coordinates with the displacement vector $\vec{u}$ having only a radial component $u(r)$ which is independent of the polar angle θ. Consistent with previous re-scaling of the elastic moduli, we also re-scale the BVP so that the wound radius is dimensionless and of unit magnitude. With a prime indicating differentiation with respect to r, $()' = d()/dr$, the BVP in this case simplifies to

$$\sigma'_{rr} + \left(\frac{E}{r}\right)\frac{u' - u/r}{1 + u' + u/r} = \frac{\lambda u}{1 + u' + u/r}, \tag{9}$$

$$r = 1: \quad \sigma_{rr} = 0, \quad r \to \infty: \quad u \to 0, \tag{10}$$

where

$$\sigma_{rr} = \frac{1}{1 + u' + u/r}\left[E u' + \Gamma\left(u' + \frac{u}{r}\right) + \frac{1}{1 + \beta\left(u' + \frac{u}{r}\right)}\right]. \tag{11}$$

Note that for a circular wound, the specified boundary conditions are consistent with global equilibrium. This is seen by integrating the differential equilibrium

equation (1) over the wound area and applying the two-dimensional divergence theorem to the stress term to get

$$\oint_{\Sigma} (\boldsymbol{\sigma} \cdot \vec{n})\, ds + \int\int_{\Omega} (\lambda \vec{u})\, dA = \vec{0},$$

where Ω is the region exterior of the circular wound edge Σ. The first integral vanishes because of the stress-free edge condition and the second vanishes because the displacement field is polarly symmetric. The same consistency holds for doubly symmetric wound area, i.e., a wound shape that is invariant under reflections through two mutually orthogonal Cartesian axes (see [9]). Considerable insight to this initial phase of embryonic epidermal wound healing has been gained from the work on the quasi-static equilibrium phase of a circular wound in [10, 11, 15, 16] (see also [2]). Numerical solutions for this problem (as well as for the problem of an asymmetrical wound not previously investigated) have also been obtained and used as initial conditions for the wound closing phase in [9].

Because of its high degree of nonlinearity, numerical solutions of the BVP (9)–(11) involve considerably more arithmetic operations and often converge rather slowly for high accuracy. For computational efficiency in generating "initial states" for the subsequent time evolution of the wound closure process and in the computation of the actual temporal evolution of a wound, it is expedient to work with a simpler elastomechanical model for the same problem during the formulation and testing stage of the wound closing model. As the wound sensing protocol is the principal concern of this paper, we will develop in the next subsection a related linear model for the quasi-equilibrium phase (and for the wound contraction phase later) to gain some computational efficiency in our elastodynamic model development. Once the dynamic wound closing model has been validated, we can restore the finite strain features in actual applications whenever appropriate.

2.2. A small strain quasi-equilibrium model

The elastic strain tensor (4) used in the constitutive relation (3) for the elastic stress tensor is the *linear strain* tensor (and not the actual strain tensor in Lagrangian or Eulerian form though more complete expressions for finite strain components have been used in other variants of the Murray–Sherratt model [2, 10]). For the purpose of developing and validating a dynamic model for the wound closing phase, we further simplify the model by the additional approximation $1 + \eta \boldsymbol{\nabla} \cdot \vec{u} \approx 1$ as long as $|\eta| = O(1)$ (and $-1 \ll \boldsymbol{\nabla} \cdot \vec{u} < 0$). For this simpler "small strain" model, we take

$$\boldsymbol{\sigma} = [E\boldsymbol{\epsilon} + \Gamma(\vec{\nabla} \cdot \vec{u})\mathbf{I}] + \boldsymbol{\sigma}^a, \tag{12}$$

where to a first approximation the *scaled* active contraction stress $\boldsymbol{\sigma}^a$ is

$$\boldsymbol{\sigma}^a = (1 - \beta\vec{\nabla} \cdot \vec{u})\mathbf{I}, \tag{13}$$

and the constant term has no role in the (vector) differential equation of equilibrium after differentiation (but is not negligible in the stress-free edge condition). The BVP (6)–(8) simplifies to

$$\vec{\nabla} \cdot \left[E\boldsymbol{\epsilon} + \Gamma(\vec{\nabla} \cdot \vec{u})\mathbf{I} + (1 - \beta\vec{\nabla} \cdot \vec{u})\mathbf{I}\right] - \lambda\vec{u} = \vec{0}, \tag{14}$$

with

$$[\boldsymbol{\sigma} \cdot \vec{n}]_{\vec{x}\varepsilon\Sigma} = [\vec{\sigma}_n]_{\vec{x}\varepsilon\Sigma} = \vec{0}, \quad [\vec{u}]_{|\vec{x}|\to\infty} \to \vec{0}, \tag{15}$$

where

$$\boldsymbol{\sigma} = E\boldsymbol{\epsilon} + \Gamma\vec{\nabla} \cdot \vec{u}\mathbf{I} + (1 - \beta\vec{\nabla} \cdot \vec{u})\mathbf{I}. \tag{16}$$

For the special case of a *circular wound* so that $\vec{u} = u(r)\hat{r}$ (where r is the radial coordinate measured from the center of the circular wound and $\hat{r}$ is the unit vector in the radial direction), the relation (14) simplifies to

$$[\sigma_{rr}]' + \frac{1}{r}(\sigma_{rr} - \sigma_{\theta\theta}) = \lambda u \tag{17}$$

and (16) simplifies to

$$\sigma_{rr} = Au' + B\frac{u}{r} + 1, \quad \sigma_{\theta\theta} = Bu' + A\frac{u}{r} + 1, \tag{18}$$

where $(\,)' = d(\,)/dr$, $B = \Gamma - \beta$ and $A = E + B$. Upon using (18) in (17), we obtain a single second order ordinary differential equation (ODE) for $u(r)$:

$$Au'' + \frac{A}{r}u' - \frac{A}{r^2}u = \lambda u. \tag{19}$$

The ODE (19) is supplemented by the two boundary conditions (10) which in view of (18) take the form

$$\left[Au' + B\frac{u}{r} + 1\right]_{r=1} = 0, \quad \lim_{r\to\infty} u(r) = 0. \tag{20}$$

The governing differential equation (19) is in the form of the differential equation for small rotationally symmetric deformations of an elastic sheet on an elastic foundation. In fact, the BVP (19) and (20) for $\beta = 0$, reduces to that for an elastic sheet on an elastic foundation subject to a rotationally symmetric edge stress distribution. The linearized theory formulated above should be adequate for sufficiently small strain deformations. If strains should not be small, we always have the option of using the Murray–Sherratt finite strain theory instead.

Recall that we have already nondimensionalized both the wound radius a and the radial displacement field by the actual wound radius and the elastic moduli E and Γ by residual stress τ_0 in the absence of actin filament compaction, while the elastic foundation parameter λ and the actin filament compaction

parameter β have been normalized by τ_0/a^2. We adopt from [3] the following values for these dimensionless parameters for a benchmark solution:

$$E = 0.5, \quad \Gamma = 0.8, \quad \beta = 0.2 \quad \lambda = 3. \tag{21}$$

Upon setting

$$b = \frac{B}{A}, \quad \Lambda^2 = \frac{\lambda}{A} \tag{22}$$

we may rewrite the BVP for the radial displacement as

$$u'' + \frac{1}{r}u' - \frac{1}{r^2}u = \Lambda^2 u \tag{23}$$

with

$$\left[u' + b\frac{u}{r} + \frac{1}{A}\right]_{r=1} = 0, \quad \lim_{r\to\infty} u(r) = 0. \tag{24}$$

The solution of the linear ODE (23) is in terms of Bessel functions. The particular solution that tends to zero as $r \to \infty$ is

$$u(r) = c_0 K_1(\Lambda r) \equiv c_0 K_1(x), \quad x = \Lambda r, \tag{25}$$

where $K_1(\cdot)$ is a modified Bessel function of order 1 [9]. The constant c_0 is chosen to satisfy the edge condition at $r = 1$:

$$c_0 = \frac{1}{A\{\Lambda K_1'(\Lambda) + bK_1(\Lambda)\}}, \quad (\,)' = \frac{d(\,)}{dx}. \tag{26}$$

Since the properties of $K_1(x)$ are well documented, not much more needs to be said about the solution for $u(r)$ as given by (25) and (26) except that from the asymptotic behavior [17]

$$\{K_1(x), K_1'(x)\} \sim O\left(\frac{e^{-x}}{\sqrt{2x/\pi}}\right) \quad \text{as} \quad x \to \infty, \tag{27}$$

we have

$$u(r) \sim \frac{e^{-\Lambda(r-1)}}{A(\Lambda + b)\sqrt{r}}. \tag{28}$$

With $\Lambda \lesssim \sqrt{3}$ for our set of parameter values, the asymptotic expression (28) should only be used for $r \gg 1$, in particular not at (or near) the edge of the wound. The actual solution of the BVP (19) and (20) has been computed numerically to provide the initial condition for the dynamic wound closing process in Section 3.

2.3. Numerical solution for circular wounds

Accurate evaluations of the exact solution (25)–(26) have been checked by using available BVP solvers on Matlab (bvp4c) and Maple (dsolve) for the BVP (23) and (24). For numerical simulations, the exterior domain (for the wounded epidermis) is approximated by a large (but finite) annular domain $\Omega_R = \{\vec{x} \mid 1 < r < R\}$ for $R \gg 1$. Agreement to four significant figures was found for the radial displacement in all cases between $R = 20$ and $R = 40$. A typical radial displacement distribution for (23) and (24) is shown in Figure 3; the distribution in space is qualitatively the same as that of (6)–(8), to be shown in Figure 4 (see also [11, 2]). Numerical differences between the results for the two models and those obtained in [11, 2] are expected since strains are not sufficiently small for the small strain model to be applicable. Hence, we should return to an appropriate finite strain model such as (9)–(11) (or (6)–(8) for more general wound shape) after the development and validation of the elastodynamics model.

Effects of the various stiffness factors are shown in Table 1 where the radial displacement at the wound edge is given for two-fold changes from the benchmark problem with the basic set of parameter values given in (21) (see also Table 3) and used for Figure 3. Not surprisingly, the displacement is larger for a more compliant epidermis or a more compliant underlying mesenchyme. However, unlike in the finite strain model, the elastostatic behavior of the wound epidermis is less sensitive to the actin filament compaction parameter β with a less than 5% change in the maximum radial displacement resulting from doubling or halving the typical value of β given in (21). Hence, results for small strain model should be used only for substantially larger values of Γ, E and λ and for β substantially below the critical value β_{cr} found in [11, 2]. For our choice of Γ and E, we have $\beta_{cr} = 0.23$.

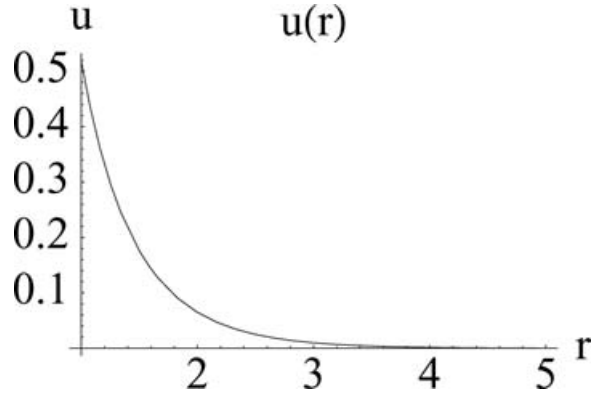

Figure 3. Radial displacement $u(r)$ of a circular wound at quasi-equilibrium as predicted by (19) and (20). Parameter values: $E = 0.5$, $\Gamma = 0.8$, $\beta = 0.2$, $\lambda = 3.0$.

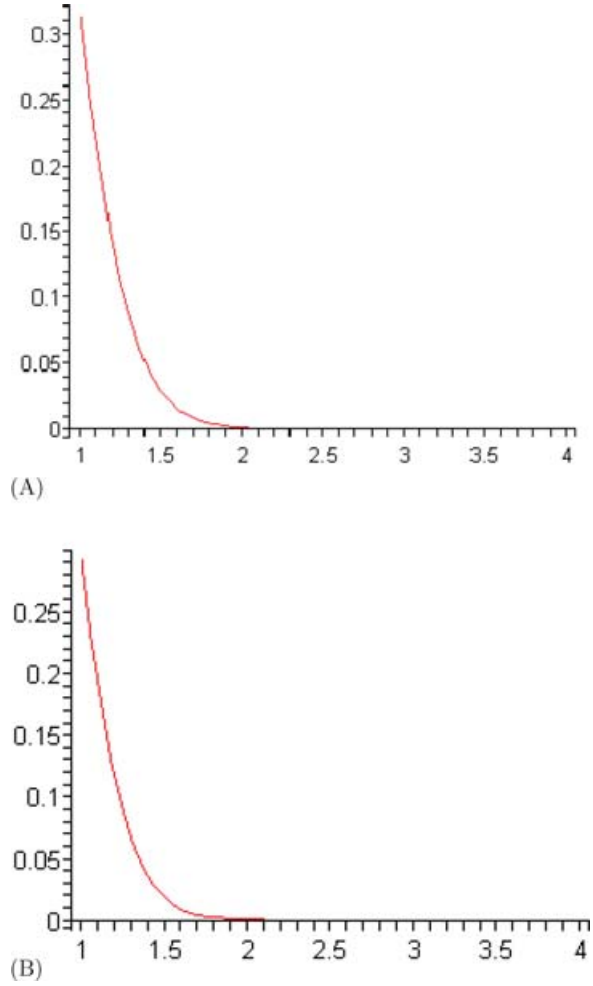

Figure 4. Radial displacement distribution for a circular wound as predicted by (6)–(8) with (A) $\beta = 0.2$ and (B) $\beta = 0.22$. Values of the other parameters in both solutions: $E = 0.5$, $\Gamma = 0.8$, $\lambda = 3.0$.

Table 1
Quasi-Equilibirum Radial Displacement at Wound Edge for Wounds with Various Parameter Values

$u(1), u'(1)$	$p/2$	p	$2p$
$p = \lambda = 3$	0.6968, −1.2892	0.5187, −1.1920	0.3780, −1.1153
$p = \beta = 0.2$	0.5055, −1.1282	0.5187, −1.1920	0.5505, −1.3558
$p = (E, \Gamma) =$ (0.5, 0.8)	0.8097, −2.5821	0.5187, −1.1920	0.3410, −0.6156

As indicated above, the corresponding BVP by the (9)–(11) variant of the Murray–Sherratt finite strain model have also been solved numerically. The use of available software such as **bvp4c** and **dsolve** for the BVP (9)–(11) requires a preliminary transformation into a form expected by these solvers. For the BVP for the small strain model (23) and (24), the expected first order system of two ODE for u and v is obtained by simply setting $v = u'$ with $u'' = v'$ given by the equilibrium equation.

For BVP (9)–(11), it appears to be simpler to let $v = u' + u/r$ or

$$u' = v - \frac{u}{r} \tag{29}$$

and write the second order ODE (9) as

$$v' = \frac{\lambda u(1+v)}{E + \Gamma + Er^{-1}u - [(1+\beta) + 2\beta v](1+\beta v)^{-2}}. \tag{30}$$

The two first order ODE (29) and (31) for u and v are supplemented by the boundary conditions (10)–(11) now re-written in terms of u and v:

$$u(R) = 0, \quad (E+\Gamma)v(1) - Eu(1) + [1+\beta v(1)]^{-1} = 0. \tag{31}$$

The BVP (29)–(31) is now in the form expected by the solvers **bvp4c** and **dsolve**.

Accurate numerical solution for (29)–(31) with absolute error of 10^{-6} have been obtained with a typical distribution of radial displacement shown in Figure 4 for $\beta = 0.20$ and $\beta = 0.22$, both less than $\beta_{cr} = 1 - (\Gamma + E)^{-1} \simeq 0.23$. As expected, the maximum displacement (at the wound edge) is smaller for the finite strain model. With $u' < 0$ being the dominant correction, the effect of the factor $(1 + u' + u/r)^{-1}$ is equivalent to increasing the elastic moduli of the epidermal sheet, stiffening the epidermis and thereby attaining a smaller radial displacement.

The fact that the difference in the maximum edge displacement is rather substantial requires that the small strain theory be used only for sufficiently small τ_0 in the active stress term (3) so that the normalized elastic moduli Γ, E, and λ are sufficiently large. Otherwise, some form of finite strain theory should be used for the quasi-equilibrium problem to give an appropriate initial condition for the closing phase of wound healing. The higher epidermis stiffness of the finite strain model also limits much of the radial displacement to a boundary layer adjacent to the wound edge.

3. Elastodynamics of wound closure

3.1. The mechanism of wound recognition

We now turn to the principal concern of this paper, the recovery process of an epidermal wound in an embryo. There is generally a shortage of data on such

wounds; nevertheless, biologists seem to agree that an embryonic epidermal wound closes via a *"purse-string" effect* [3]. While there is an intuitive understanding of this mechanical analogy, there appears to be no generally accepted theory on how it may induce an embryonic epidermal wound to close and heal (see, however, the review [18]). We will formulate a "wound closure postulate" below to transform this vague notion of purse-string effect into a biomechanical process of actin re-alignment and contraction for wound closing (resulting in a purse-string effect). As a first step toward this wound closing mechanism, we need to characterize how an organism recognizes the presence of a wound.

There is evidence that cells injured by wound infliction release chemicals that signal to other cells to change their genetic and locomotive behavior in certain ways. However, the significance of chemotaxis, that is, the phenomenon of cells traveling in response to a chemical signal, in embryonic wound healing is still unclear, as is the relation between chemotaxis and the purse-string mechanism. Chemotaxis is believed to be based on the cells' response to chemo-attractant concentration gradients in extracellular environment which diffuse away in a matter of minutes (or tens of minutes at most). This is the same time scale as that of the formation of the actin purse string mentioned above. Since concentration gradients have a well-defined direction, they carry enough information to orient and align the actin filaments perpendicularly to the concentration gradients so that the purse string is formed. One may conjecture that the relation between gradients and actin alignment is that of cause and effect, but this is not crucial to our wound closing model formulation. The evolution of wound closure begins at the instant when the quasi-equilibrium described in the previous section has just been reached. By this time, the "purse string" has already been formed and the chemo-attractant gradients, having played their role, have already diffused. There are now two possibilities: either the gradients have no further effect, or their brief presence has started some chain reaction which continues after they are gone.

In this paper, we confine ourselves to the first possibility, based on the following consideration. Unless the hypothetical chain reaction is sufficiently long-lasting or furnished with excellent feedback control, its role in wound recovery can be shown insubstantial by the following thought experiment: keep a wound open by mechanical means until the reaction dies out, remove the mechanical constraint against closure, and we still expect the wound to close. (As an example, we have surgeon-inserted drainage devices but the wound would still close after their removal at some later time.) Hence, the class of dynamic models of wound closing formulated below will rest on the assumption that the chemo-attractant gradients, once diffused, have no further bearing on wound recovery. We will also assume in our models that actin filaments re-structure themselves only through actin filament response to the detection of wound shape change.

3.2. Equations of epidermal motion

An important component of a theory of wound closing is a wound recognition by way of a cell-to-cell signaling mechanism. To see the various considerations that go into a quantitative theory of wound recognition and cell–cell signaling, we first formulate the equation of motion for the closing phase of the wounded epidermis. Our class of epidermal models is concerned with a continuum of epidermal cells occupying a domain M in R^2, given the relatively small thickness of the epidermis compared to its other dimensions (so that we have a thin sheet or across-thickness average model). For simplicity, M is taken to be all of R^2 prior to wound infliction and the cell mass (area) density of the epidermis is taken to be uniform and normalized to unit value. Upon the infliction of a wound over a simply connected part Ω_w of the epidermis with a boundary curve Σ, the region Ω outside the wounded area (with $\bar{\Omega} \cup \bar{\Omega}_w = R^2$) undergoes deformation within R^2 with the edge of the wound retracting until it reaches a quasi-static equilibrium configuration and the wound closing process begins. We identify an infinitesimal cell mass by its location specified by the plane Cartesian coordinate vector $\vec{x} = (x_1, x_2)$ before deformation caused by the wound. At any instance after the onset of deformation, cell mass originally located at $\vec{x}$ has been displaced to location $\vec{c}(\vec{x}, t) = \vec{x} + \vec{u}(\vec{x}, t)$, again in R^2, with a plane displacement vector $\vec{u}(\vec{x}, t)$ defined for all points in Ω. In our class of models, we take the cell area mass density to remain unit throughout assuming sufficient cells produced (or destroyed) to adequately support this approach.

The vector equation of motion for the cell displacement vector $\vec{u}(\vec{x}, t)$ is effectively known from classical elastodynamics. The additional restoring force due to the underlying mesenchyme attachment previously in the form of $\lambda\vec{u}/(1 + \nabla \cdot \vec{u}) \simeq \lambda\vec{u}$ for the small strain elastostatic case is now modified to include the effect of the underlying mesenchyme which moves with the contracting epidermis *at a rate proportional to the velocity* [3] so that we have

$$\partial_{tt}\vec{u} = \nabla \cdot \boldsymbol{\sigma} - \lambda(\vec{u} + c_m \partial_t \vec{u}), \quad \partial_t(\,) = \frac{\partial(\,)}{\partial t}. \tag{32}$$

Here we have taken the surface epidermal mass density to be unit. The coefficient λc_m characterizes the strength of the mesenchymal motile response, reflecting the experimentally observed movement of the mesenchyme together with the epidermis during the re-epithelialization of the wound area [3]. The stress tensor is related to the strains experienced by the wounded epidermis in recovery and in turn to the displacement components by way of the strain displacement relations.

A critical aspect of the elastodynamic formulation of the problem is the constitutive relations expressing the stress components in terms of the strain and strain rate components. We take these in a Kelvin–Voigt form

$$\boldsymbol{\sigma} = \mu_1 \partial_t \boldsymbol{\epsilon} + \mu_2 \partial_t (\nabla \cdot \vec{u}) \mathbf{I} + E\boldsymbol{\epsilon} + \Gamma(\nabla \cdot \vec{u})\mathbf{I} + \boldsymbol{\sigma}^a, \tag{33}$$

where the strain tensor $\boldsymbol{\epsilon}$ is given in terms of $\vec{u}$ by (4). The additional parameters μ_1, μ_2 are coefficients of viscosity for which the values given in Table 3 are taken from [19]. The active stress tensor $\boldsymbol{\sigma}^a$ is associated with actin filament contraction, an important new element in the embryonic epidermal wound problem. The key to the whole dynamic model of wound closure is an appropriate specification of $\boldsymbol{\sigma}^a$. For this specification, we need to discuss how cells sense the presence of a wound and move toward it for healing. We will discuss this recognition process in the next subsection and then return to complete the partial differential equation (PDE) of epidermal motion afterwards.

3.3. Cell-to-cell signaling

Suppose $\vec{c}^{(k)} = \vec{c}(\vec{x}^{(k)}, t)$, $k = 1, 2$, are deformed positions of two cell mass points originally at the two distinct locations $\vec{x}^{(1)}$ and $\vec{x}^{(2)}$. Suppose, further, that $\vec{c}^{(1)}$ (resp., $\vec{c}^{(2)}$) is near (resp., far from) the edge of the wound in the deformed configuration. It is known from [3] that these two cell mass points will then exhibit different behaviors. Immediately before wound infliction, both cells have the same biological functions, i.e., they have the appropriate genes expressed to roughly equal degrees. The differences in behavior emerges, under the above suppositions, after wound infliction. It is therefore reasonable to suppose that these differences are caused by the differences in some external wound-generated signals received by the cell masses in different locations.

To incorporate this spatial (locational) difference in cell behavior in the formulation of the active stress, we introduce a non-negative scalar *interaction function between two cell mass points* $\vec{c}^{(m)}$ and $\vec{c}^{(n)}$, denoted by $F(\vec{c}^{(m)}, \vec{c}^{(n)})$, which is non-increasing in $|\vec{c}^{(m)} - \vec{c}^{(n)}|$. A simple class of such an interaction functions is

$$F\big(\vec{c}^{(m)}, \vec{c}^{(n)}\big) = g\big(\big|\vec{c}^{(m)} - \vec{c}^{(n)}\big|\big) \geq 0,$$

where $g(\cdot)$ is a non-increasing scalar function of a real non-negative variable. (The special case of $g(\zeta) \propto \zeta^{-2}$ would be analogous to Newton's inverse square law of gravitational attraction.) More general choices of an interaction function may include the concentration of a chemical nutrient leaking out of the injured cells as a significant factor in the healing process. An appropriate choice of the interaction function $F(\vec{c}^{(m)}, \vec{c}^{(n)})$ ultimately depends on the type of intercellular signals that it is to reflect.

The basic known signal types and their characteristics are listed in Table 2 [20, 21]. For the first type of signals listed in the table to arise, the organism must be relatively mature: neural networks require that sufficiently many cells have differentiated to become neurons. The endocrine system, in turn, requires a vascular network which, however well developed, cannot conduct signals in a

Table 2
Basic Known Cell Signal Types

Signal Type	Carrier	Channel	Range	Speed
neural	electrical impulse	axon channels	long	$\sim$ light
endocrine	hormones	blood	vascular	blood flow
paracrine	chemical nutrient	extracellular	local	2-D diffusivity
direct contact	ions, etc.	connexons	local	1-D diffusivity
mechanical	mechanical waves	tensile fibers	long	waves

well-defined rectilinear way. Contact signaling takes place at every instant, but acts short-range. Our numerical evidence, on the other hand, suggests that a long-range signal type is required for the wound to close. These considerations narrow the possibilities to the remaining two signal types.

Paracrine signaling can play a role immediately after the wound has been inflicted: chemo-attractants leak out of the injured cells, giving rise to a concentration gradient pointing toward the wound. This may well be the cause of the actin "pure string" formation that occurs shortly after wounding [3, 1]. The gradients then diffuse away, and it is not clear whether the ensuing wound closure is primarily (a) a sequence of events set in motion by the chemo-attractant concentration gradients, or (b) a response to other signals present. In this paper, we choose to explore possibility (b) (keeping in mind that the wound closing process is to start after the "purse string" has already been formed), which rules out paracrine signaling in our models.

More specifically, we adopt the position that wound closure is driven by signals with a precisely defined direction and a long range of propagation without effects from injured cell-generated nutrients, leading to an alignment of actin filaments and a purse-string type contraction. These properties are observed in signals of the last type listed in Table 2, the mechanical type signals [21]. For the present paper, we limit ourselves to the very simple case of

$$g(\zeta) = H(r_{sp} - \zeta) := \begin{cases} 1 & (0 \le \zeta \le r_{sp}) \\ 0 & (r_{sp} < \zeta < \infty) \end{cases}$$

so that

$$F\big(\vec{c}^{(m)}, \vec{c}^{(n)}\big) = H\big(r_{sp} - \big|\vec{c}^{(m)} - \vec{c}^{(n)}\big|\big), \tag{34}$$

where both cell mass points lie outside the wound area, i.e., $\vec{c}^{(k)} \in \Omega$, $k = m, n$, and are not one and the same cell, as a cell is assumed to be unresponsive to its own signals. The latter qualification could have been incorporated into (34) mathematically by adding a term $-H(r_{cd} - |\vec{c}^{(m)} - \vec{c}^{(n)}|)$ to the expression for $F(\vec{c}^{(m)}, \vec{c}^{(n)})$. However, the effect of such an added term would be negligible given the small linear dimension of an epidermal cell.

The cell–cell interaction function F in (34) was chosen for its relative simplicity (in addition to phenomenological appropriateness) which will help minimize the required computations in our wound closing model. It may be replaced by other (possibly more realistic) cell–cell interaction without affecting the efficacy of our approach to modeling wound closing.

3.4. Biosignal asymmetry vector and active stress

In our class of models, a cell is expected to be able to distinguish between directions from which it receives signals, a hypothesis supported by experimental evidence on intercellular communication for many kinds of signals [20]. To incorporate this directional effect, we define a *total biosignal* $w(\vec{c}, \hat{y})$ *received by* $\vec{c}$ *from (all cells in) direction* $\hat{y}$ by summing the contributions $F(\vec{c}, \vec{c}^*)$ of all $\vec{c}^*$ in the $\hat{y}$ direction:

$$w(\vec{c}, \hat{y}) := \int_0^\infty F(\vec{c}, \vec{c} + s\hat{y})\, ds, \tag{35}$$

where $\hat{y}$ is a unit vector. We refer to such a signal as *the* $\hat{y}$*-biosignal at* $\vec{c}$. Such a signal can be averaged over all directions $\hat{y}$ to yield *the average biosignal* $\bar{w}(t, \vec{c})$ *received at* $\vec{c}$. Finally, for each direction $\hat{y}$, we consider the difference

$$\phi(t, \vec{c}, \hat{y}) := \bar{w}(t, \vec{c}) - w(\vec{c}, \hat{y}), \tag{36}$$

which measures at $\vec{c}$ the deviation of the $\hat{y}$-biosignal from the average biosignal $\bar{w}(t, \vec{c})$. We call $\phi(t, \vec{c}, \hat{y})$ the *biosignal asymmetry of* $\vec{c}$ *in the* $\hat{y}$ *direction*. Upon integrating $\phi(t, \vec{c}, \hat{y})\hat{y}$ over all the directions $\hat{y}(\theta)$ that emanate from $\vec{c}$ at time t, we obtain the *mean biosignal asymmetry vector*

$$\vec{\Phi}(t, \vec{c}) := \int_0^{2\pi} \phi(t, \vec{c}, \hat{y})\hat{y}(\theta)\, d\theta. \tag{37}$$

The following observation limits the range of influence of wound signal and thereby its contribution to the active stress:

PROPOSITION 1. *At a point* $\vec{c}$ *sufficiently far away from the wound at time t, we have* $\vec{\Phi}(t, \vec{c}) = \vec{0}$.

Proof: For a fixed t, if the points $\vec{c}$ and $\vec{c}^*$ are both outside the wound and within distance r_{sp} of each other, then our choice of F implies that

$$F(\vec{c}, \vec{c}^*) = 1.$$

Thus, if the wound and the disc of radius r_{sp} centered at $\vec{c}$ intersect in a set of area zero (including the case when this set is empty), then the average $\bar{w}(t, \vec{c})$ coincides with $w(t, \vec{c}, \vec{c} + s\hat{y})$ for $0 \le s \le r_{sp}$. Thus, the expression

$\phi(t, \vec{c}, \hat{y})$ under the integral in (37) is zero identically for all θ. This completes the proof. ■

The mean biosignal asymmetry vector $\vec{\Phi}(t, \vec{c})$ plays a central role in determining the stresses in the wounded epidermis to complete the formulation of our elastodynamic model of wound closing. Along with the conventional elastic and visco-elastic stresses (designated as the *passive stresses* in our model), an epidermis experiences additional stresses generated by the observed directional realignment and contraction of the actin filaments. For the specification of this new type of stresses, designated as *active stresses* $\boldsymbol{\sigma}^a(\vec{x}, t)$ herein, we adopt the following three-part *active stress postulate*:

The active stress postulate

1. In an intact epidermis, the corresponding active stresses have no preferred direction (with biosignal asymmetry identically zero) and hence consist only of a constant hydrostatic pressure in space, equal to $\boldsymbol{\sigma}^{a,0} = \mathbf{I}$ after re-scaling.
2. In the presence of a wound with a nonzero biosignal asymmetry field $\vec{\Phi}$, actin filaments contract in directions orthogonal to the mean biosignal asymmetry vector $\vec{\Phi}(t, \vec{c})$, at a rate that increases with $|\vec{\Phi}|^2$.
3. The rate of change of $\boldsymbol{\sigma}^a(\vec{x}, t)$ is proportional to the difference of $\boldsymbol{\kappa} - \boldsymbol{\sigma}^a$ where $\boldsymbol{\kappa}$ is the perturbation of $\boldsymbol{\sigma}^{a,0}$ by the actin filament contraction, which is $c_\phi(\vec{\Phi}^\perp \otimes \vec{\Phi}^\perp)$ according to item 2 above with $\vec{\Phi}^\perp$ being the image of $\vec{\Phi}$ under a 90^o clockwise rotation.

From this three-part postulate, we have for the evolution of $\boldsymbol{\sigma}^a$ the following differential equation:

$$\partial_t \boldsymbol{\sigma}^a = \mu_a \{\boldsymbol{\sigma}^{a,0} - \boldsymbol{\sigma}^a + c_\phi(\vec{\Phi}^\perp \otimes \vec{\Phi}^\perp)\}, \tag{38}$$

where μ_a and c_ϕ are positive constants determined by experiments. Note that if $\vec{\Phi} = \vec{0}$ (such as in the case of no wound inflicted or when $\vec{c}$ is outside the range $1 < |\vec{c}| < r_{sp}$), then (38) merely maintains its initially undeformed state: $\boldsymbol{\sigma}^a = \boldsymbol{\sigma}^{a,0} = \mathbf{I}$ (and the hydrostatic pressure $\boldsymbol{\sigma}^{a,0}$ is therefore a unique stable equilibrium configuration of the active stress).

A simple example illustrating the effect of (38) for $\vec{\Phi} \neq \vec{0}$ is the rotationally symmetric case to be discussed in the next section. Note that our mechanism for an organism to continue to detect and close a wound after the purse string of actin filaments has been formed at quasi-equilibrium is necessarily phenomenological (and not founded on any specific biological process) at this stage of the theoretical development. A biological process based model would require more information on the underlying biological mechanism for this part of the biological phenomenon.

The PDE–ODE system (32)–(38) is supplemented by

- the boundary conditions (7) and (8) requiring the (updated) wound edge to be free of stress and quiescence at infinity (or, for the purpose of numerical solutions, at some large circle Σ_R of radius R surrounding the wound), and
- the initial conditions

$$t = 0: \quad \vec{u} = \vec{u}^{qe}(\vec{x}), \quad \partial_t \vec{u} = \vec{0}, \quad \boldsymbol{\sigma}^a = (\boldsymbol{\sigma}^a)^{qe}, \tag{39}$$

where $\vec{u}^{qe}$ and $(\boldsymbol{\sigma}^a)^{qe}$ are from the solution of the BVP (6)–(8) for the quasi-equilibrium state of Section 2 or its small strain counterpart for which $\boldsymbol{\sigma}^a$ is known from (13) to be $(\boldsymbol{\sigma}^a)^{qe} = (1 - \beta \nabla \cdot \vec{u}^{qe})\mathbf{I}$.

In summary, the elastodynamics of epidermal wound closing is governed by the vector differential equations of motion (32) and (38), the boundary conditions (7) and (8) and the initial conditions (39). The (scaled) viscoelastic and biological parameters appearing in these equations are listed in Table 3, each assigned a numerical value for our bench mark wound. For the elastic and biological parameters E, Γ, λ, and β already encountered in the quasi-static model, we use the scaled values given in Section 2 (which, in turn, were taken from [2]). For the parameters characterizing the viscosity and cell-signal transduction properties of the tissue, there are no experimental results on their values; we will offer a set of reasonable value ranges for actual numerical simulations. For the choices indicated in Table 3, a wound that closes does so within one unit of the time variable in the model. The available experimental evidence suggests that an embryonic epidermal wound closes in about 20 hours (see [2] and references therein). Thus, one unit of the scaled time t in the model equation above corresponds to 20 hours.

Table 3
Parameter Value Used in the Benchmark Wound

Coefficient	Physical Parameter	Value
μ_1	Shear viscosity	1.0
μ_2	Bulk viscosity	0.1
$E/2$	Shear modulus	0.25
Γ	Lame constant	0.8
λ	Mesenchyme spring force constant	3.0
λc_m	Mesenchyme motility modulus	0.3
μ_a	Actin cable contraction parameter	1.0
c_ϕ	Biosignal intensity	100
β	Actin compaction rate constant	0.2
r_{sp}	Mechanical signal propagation range	2.0

3.5. An efficient algorithm for $\vec{\Phi}(t, \vec{c})$

In the differential equation (32), $\boldsymbol{\sigma}$ is given in terms of the strain measures (see (4)) and the active stress by (33). The active stress tensor $\boldsymbol{\sigma}^a$ is, in turn, determined by the evolutionary equation (38) involving the biosignal asymmetry vector $\vec{\Phi}(t, \vec{c})$. As long as $\vec{c}$ is at a distance less than r_{sp} from the wound edge (so that we have $\vec{\Phi} \neq \vec{0}$), the definition of $\vec{\Phi}(t, \vec{c})$ through (35)–(37) involves double integration over a different complex geometrical region for each $\vec{c}$ (which changes with time). An efficient discrete time algorithm for computing $\vec{\Phi}(t, \vec{c})$ for different $\vec{c}$ is needed to make numerical simulations practical. For such an algorithm, we introduce the notation $E_i(t)$ to denote the extent of the intact epidermis at time t:

$$E_i(t) := \{\vec{x} + \vec{u}(\vec{x}, t) \,|\, \vec{x} \in \Omega\},$$

where Ω is the physical domain corresponding to the unwounded portion of the epidermis prior to onset of any deformation, quasi-static or dynamic.

Next, we note that for our interaction function $F(\vec{c}, \vec{c}^*)$, there is a cutoff at r_{sp} (see (34)) for the reach of the biosignal from the cell mass at any location $\vec{c}$ so that we may write

$$w(\vec{c}, \hat{y}) = \int_0^{r_{sp}} F(\vec{c}, \vec{c} + s\hat{y})\, ds,$$

where

$$F(\vec{c}, \vec{c}^*) = \begin{cases} 1 & \text{if } \vec{c} \text{ and } \vec{c}^* \text{ are in } E_i(t) \text{ and within distance } r_{sp} \text{ of each other} \\ 0 & \text{otherwise.} \end{cases}$$

Consequently, the average biosignal at $\vec{c}$ is given by

$$\bar{w}(t, \vec{c}) := \begin{cases} \displaystyle\int\int_{|\vec{c}-\vec{\xi}| \leq r_{sp}} F(\vec{c}, \vec{\xi})\, dA = 0 & \text{if } \vec{c} \in E_i^C(t) \\ A_c(t) & \text{otherwise,} \end{cases}$$

where $E_i^C(t)$ is the complement of $E_i(t)$ and A_c is area of the intersection of the circular disc $D_c(t, \vec{c}) = \{\vec{\xi} \,|\, |\vec{c} - \vec{\xi}| \leq r_{sp}\}$ and the intact epidermis $E_i(t)$. We denote the intersection region by

$$U^c(t, \vec{c}) = D_c(t, \vec{c}) \cap E_i(t), \text{ with } A_c(t) = Area(U^c(t, \vec{c})).$$

The proposition below follows from (36) and (37).

PROPOSITION 2. *For $\vec{c}$ outside the wound area at time t, we have*

$$\vec{\Phi}(t,\vec{c}) := \int_0^{2\pi} [A_c(t) - w(\vec{c},\hat{y})]\hat{y}(\theta)\,d\theta$$
$$= -\int_0^{2\pi} w(\vec{c},\hat{y})\hat{y}(\theta)\,d\theta.$$

A very useful consequence of the result above for the development of our efficient algorithm for computing $\vec{\Phi}(t,\vec{c})$ is the following corollary:

COROLLARY 1. *If $\vec{c}$ lies outside the wound area at time t, then the point $\vec{c} - \vec{\Phi}(t,\vec{c})$ is the barycenter (center of mass) of the set $U^c(t,\vec{c})$. The latter can be calculated from the area and the center of mass of the set*

$$U(t,\vec{c}) = \{\vec{\xi}\,||\vec{c} - \vec{\xi}| \le r_{sp}\} \cap \{\textit{wound region at time } t\}$$
$$= D_c(t,\vec{c}) \cap E_i^C(t).$$

Corollary 1 reduces the computation of $\vec{\Phi}(t,\vec{c})$ to calculating the area and the barycenter of the region $U(t,\vec{c})$. We will see how this is done for the special case of a circular wound in the next section.

4. Elastodynamics of a circular wound

As an application of the general theory developed in Section 3, we consider the case of a circular wound in the sense of Section 2. In this case, the corresponding biosignal asymmetry vector field $\vec{\Phi}$ turns out to have the same polar symmetry. A proof of this property for our choice of interaction function $F(\vec{c}^{(m)},\vec{c}^{(n)})$ and its consequence for the initial-boundary value problem given below provide the key results for this class of wound problems. (The same property can be proved for a general interaction function [9].) Numerical results on the wound closing process will be computed with the help of these results. They will be presented below to demonstrate the efficacy of the elastodynamic theory for wound closing developed herein.

4.1. Polar symmetry of mean biosignal asymmetry vector

Let G be the group of operations $\boldsymbol{R}$ for vector and tensor fields defined in R^2 consisting of rotations about the origin and reflections through lines passing through the origin. The vector and tensor fields are said to be *rotationally symmetric* if they are invariant under the action of G. For radially symmetric deformation for which the displacement vector takes the form $\vec{u}(\vec{x},t) = u(r,t)\hat{r}$, we have

$$\vec{u}(\boldsymbol{R}\vec{x},t) = u(r,t)\boldsymbol{R}\hat{r} = \boldsymbol{R}[u(r,t)\hat{r}] = \boldsymbol{R}\vec{u}(\vec{x},t).$$

PROPOSITION 3. *For a rotationally symmetric deformation of a circular wound, the mean biosignal asymmetry vector (37) is invariant under the action of G, so that $\boldsymbol{R}\vec{\Phi}(t,\vec{c}) = \vec{\Phi}(t,\boldsymbol{R}\vec{c})$ for all $\boldsymbol{R}$ in G.*

Proof: For the interaction function $F(\vec{c}^{(m)},\vec{c}^{(n)})$ given in (34), it is clear that its value is not affected by the action of $\boldsymbol{R}$ on the relevant vectors:

$$\begin{aligned} F\left(\boldsymbol{R}\vec{c}^{(m)},\boldsymbol{R}\vec{c}^{(n)}\right) &= H\left(r_{sp} - \left|\boldsymbol{R}\vec{c}^{(m)} - \boldsymbol{R}\vec{c}^{(n)}\right|\right) \\ &= H\left(r_{sp} - \left|\vec{c}^{(m)} - \vec{c}^{(n)}\right|\right) = F\left(\vec{c}^{(m)},\vec{c}^{(n)}\right) \end{aligned}$$

for any pair $\{\vec{c}^{(m)},\vec{c}^{(n)}\}$. It follows from the definition of average biosignal that we have $\bar{w}(t,\boldsymbol{R}\vec{c}) = \bar{w}(t,\vec{c})$.This in turn implies

$$\begin{aligned} \boldsymbol{R}\vec{\Phi}(t,\vec{c}) &= \boldsymbol{R}\int_0^{2\pi} \phi(t,\vec{c},\hat{y})\hat{y}(\theta)\,d\theta \\ &= \boldsymbol{R}\int_0^{2\pi} \{\bar{w}(t,\vec{c}) - w(\vec{c},\hat{y})\}\hat{y}(\theta)\,d\theta \\ &= \int_0^{2\pi}\left\{\bar{w}(t,\vec{c}) - \int_0^{\infty} F(\vec{c},\vec{c}+s\hat{y})\,ds\right\}\boldsymbol{R}\hat{y}(\theta)\,d\theta \\ &= \int_0^{2\pi}\left\{\bar{w}(t,\boldsymbol{R}\vec{c}) - \int_0^{\infty} F(\boldsymbol{R}\vec{c},\boldsymbol{R}\vec{c}+s\boldsymbol{R}\hat{y})\,ds\right\}\boldsymbol{R}\hat{y}(\theta)\,d\theta \\ &= \int_0^{2\pi}\left\{\bar{w}(t,\boldsymbol{R}\vec{c}) - \int_0^{\infty} F(\boldsymbol{R}\vec{c},\boldsymbol{R}\vec{c}+s\hat{z})\,ds\right\}\hat{z}(\theta)\,d\theta = \vec{\Phi}(t,\boldsymbol{R}\vec{c}). \end{aligned}$$

This completes the proof. ■

As one consequence of the proposition above, we have the following corollary:

COROLLARY 2. *For the interaction function (34), the mean biosignal asymmetry vector has the form*

$$\vec{\Phi}(t,\vec{c}) = \begin{cases} 0 & \text{if } \vec{c} \in E_i^C(t) \\ -|\Phi(t,|\vec{c}|)|\hat{c} & \text{otherwise,} \end{cases}$$

where $\hat{c} = \vec{c}/|\vec{c}|$ is the unit vector (at the origin) in the direction of $\vec{c}$.

Proof: Let $\boldsymbol{R}_{\vec{c}}$ be a reflection through the line $\alpha\hat{c}$ for a real number α. Then $\boldsymbol{R}_{\vec{c}}\vec{c} = \vec{c}$ so that

$$\vec{\Phi}(t,\vec{c}) = \vec{\Phi}(t,\boldsymbol{R}_{\vec{c}}\vec{c}) = \boldsymbol{R}_{\vec{c}}\vec{\Phi}(t,\vec{c}),$$

where Proposition 3 is used for the second equality. This shows that $\vec{\Phi}(t, \vec{c})$ is colinear with $\vec{c}$ given the following expression for $\vec{\Phi}(t, \vec{c})$:

$$\vec{\Phi}(t, \vec{c}) = \pm|\vec{\Phi}(t, \vec{c})|\hat{c}.$$

The sign is then determined to be negative by Proposition (2). ■

4.2. The initial-boundary value problem

We consider here a circular wound region of unit radius centered at the origin. The remaining uninjured epidermis occupies the region exterior to the unit circle, $\Omega = \{\vec{x} \mid 1 < r < \infty\}$ with $r = |\vec{x}|$ being the radial coordinate of $\vec{x}$ in the conventional polar coordinate system. Given the rotational symmetry, we expect and seek a solution of the initial-boundary value with $\vec{u}$ having only a radial component independent of the polar angle θ, and with $\boldsymbol{\sigma}^a$ having a diagonal matrix $[\boldsymbol{\sigma}^a]_{(r,\theta)}$ in the polar coordinates (r, θ), with the entries also independent of θ. This last observation is a consequence of

$$\vec{\Phi}^{\perp}(t, \vec{c}) \otimes \vec{\Phi}^{\perp}(t, \vec{c}) = |\vec{\Phi}(t, \vec{c})|^2(\hat{c}^{\perp} \otimes \hat{c}^{\perp}) = |\vec{\Phi}(t, \vec{c})|^2(\hat{\theta} \otimes \hat{\theta}),$$

where $\hat{\theta}$ is the unit vector forming an orthogonal triad with the remaining two unit directional vectors $\hat{r}$ and $\hat{z}$ in the usual cylindrical coordinate system so that $\hat{r} \times \hat{\theta} = \hat{z}$. It follows that

$$\vec{u} = u(r, t)\hat{r}, \quad [\boldsymbol{\sigma}^a]_{(r,\theta)} = \begin{bmatrix} \sigma^a_{rr}(r, t) & 0 \\ 0 & \sigma^a_{\theta\theta}(r, t) \end{bmatrix}.$$

Accordingly, the velocity vector $\vec{v}$ takes the form

$$\vec{v} = v(r, t)\hat{r} = (\partial_t u)\hat{r}.$$

In numerical simulations, we will work with an approximate exterior domain $\Omega_R = \{\vec{x} \mid 1 < r < R\}$ for a sufficiently large $R(\gg 1)$ instead of Ω.

For a rotationally symmetric wound, the vector equation of motion (32) reduces to the following scalar equation for $u(r, t)$:

$$\left.\begin{aligned} \partial_{tt} u &= \hat{r} \cdot (\nabla \cdot \boldsymbol{\sigma}) - \lambda(u + c_m \partial_t u) \\ &= \sigma'_{rr} + \frac{1}{r}(\sigma_{rr} - \sigma_{\theta\theta}) - \lambda(u + c_m \partial_t u) \end{aligned}\right\}, \tag{40}$$

where the stress components given by (33) become

$$\sigma_{rr} = E\partial_r u + \Gamma\left(\partial_r u + \frac{u}{r}\right) + \mu_1 \partial_t (\partial_r u) + \mu_2 \partial_t \left(\partial_r u + \frac{u}{r}\right) + \sigma^a_{rr}$$

$$\sigma_{\theta\theta} = E\frac{u}{r} + \Gamma\left(\partial_r u + \frac{u}{r}\right) + \mu_1 \partial_t \left(\frac{u}{r}\right) + \mu_2 \partial_t \left(\partial_r u + \frac{u}{r}\right) + \sigma^a_{\theta\theta},$$

where the components of active stress tensor determined by (38) now correspond to the two scalar equations:

$$\partial_t \sigma^a_{rr} = \mu_a\left(\sigma^{a,0}_{rr} - \sigma^a_{rr}\right) = \mu_a\left(1 - \sigma^a_{rr}\right), \tag{41}$$

$$\begin{aligned}\partial_t \sigma^a_{\theta\theta} &= \mu_a\left(\sigma^{a,0}_{\theta\theta} - \sigma^a_{\theta\theta} + c_\phi\left|\vec{\Phi}^\perp\right|^2\right)\\ &= \mu_a\left(1 - \sigma^a_{\theta\theta} + c_\phi\left|\vec{\Phi}^\perp\right|^2\right).\end{aligned} \tag{42}$$

Note that the sole effect of the vector field $\vec{\Phi}$ is to increase the tangential component of the active stress.

The differential equations (40)–(42) are supplemented by the boundary conditions (7) and (8) and the initial conditions (39) which simplify to

$$t = 0: \begin{cases} u = u^{qe}(r), & \partial_t u = 0,\\ \sigma^a_{rr} = \left(\sigma^a_{rr}\right)^{qe}, & \sigma^a_{\theta\theta} = \left(\sigma^a_{\theta\theta}\right)^{qe}, \end{cases} \tag{43}$$

where a superscript "qe" denotes quantities associated with the quasi-equilibrium state of the wound. In the actual computations, to illustrate the use of the elastodynamic model, we have, for expediency, taken the quasi-equilibrium active stresses to be those for the small strain theory of Subsection 2.2:

$$\left(\sigma^a_{rr}\right)^{qe} = 1 - \beta\left(\partial_r u^{qe} + \frac{1}{r}u^{qe}\right) = \left(\sigma^a_{\theta\theta}\right)^{qe}.$$

Since the initial-boundary value problem can only be solved numerically, we also approximate the limiting condition away from the wound center by

$$u(R, t) = 0$$

for some sufficiently large value of $R \gg 1$ (instead of transforming it to a singular problem for a finite domain).

4.3. Numerical simulations

Some sample numerical results from the dynamic model developed herein are shown in Figures 5 and 6 for a circular wound of unit radius and for the parameter values given in Table 3. Figure 5 shows distributions of the radial displacement as a function of the radial position from the wound center for different normalized elapsed times from the onset of the wound closing process up to $t = 0.7$. Though not shown here, $r + u(r, t)$ is found to be positive and monotone in r for all t values computed even if the computed radial displacement $u(r, t)$ is not monotone for later times. Figure 5 gives the radial displacement at wound edge at different elapsed times starting from quasi-equilibrium; it is a more explicit indication of the wound closing as a function of time.

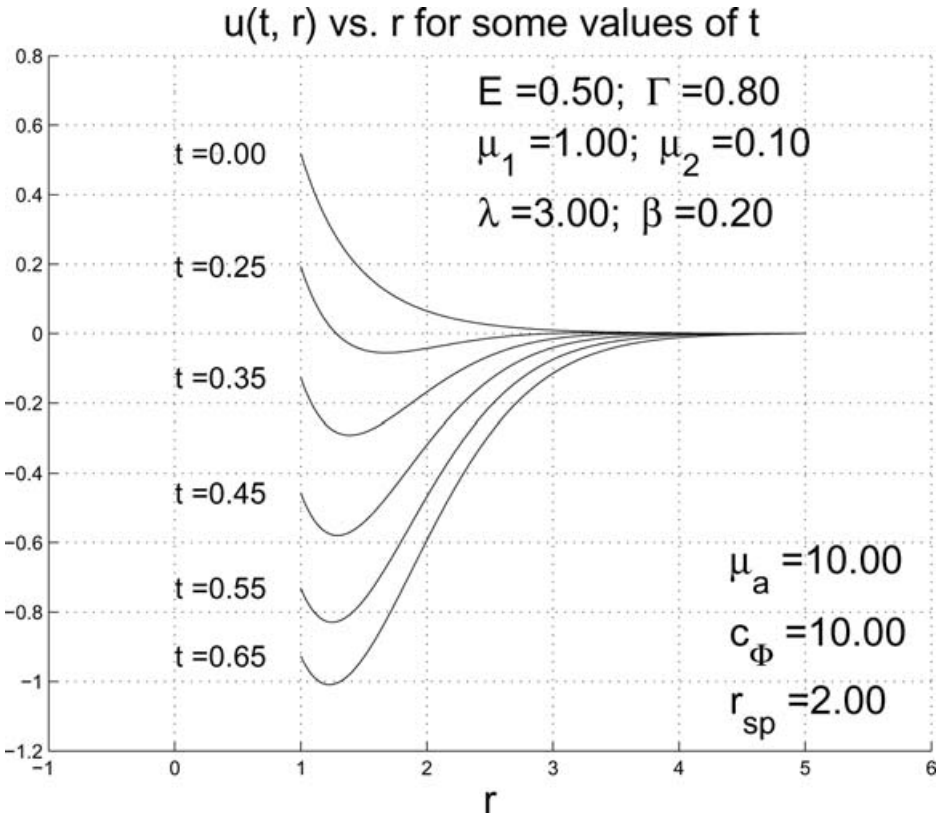

Figure 5. Distribution of radial displacement at different time instants during wound closure.

Even with just the results presented in these two figures, we have already accomplished an important objective. Numerical simulations of our viscoelasto-dynamic model using parameter values available in the literature have demonstrated the feasibility of wound closing in a model based on what we believe to be a plausible biological mechanism. It is seen from the graph of $u(1, t)$ in Figure 6 that the wound is nearly closed at $t = 0.7$ (with the wound closed at $u = -1$). While the closing process can be (and has been) computed for later times, the results are not likely to be meaningful for two reasons. The expected stress concentration phenomenon would eventually lead to high stress magnitude that necessitates a model not based on small strain approximations. More importantly, other biological process including cell differentiation and proliferation may become the dominant mechanism for closing the wound.

For a lack of data on the biosignal intensity factor c_ϕ, the actin compaction rate constant c_m, and the mechanical signal propagation range r_{sp}, we have adjusted the values of these parameters to achieve wound closing. Epidermal wounds in embryos have the unique characteristic that they close rather quickly,

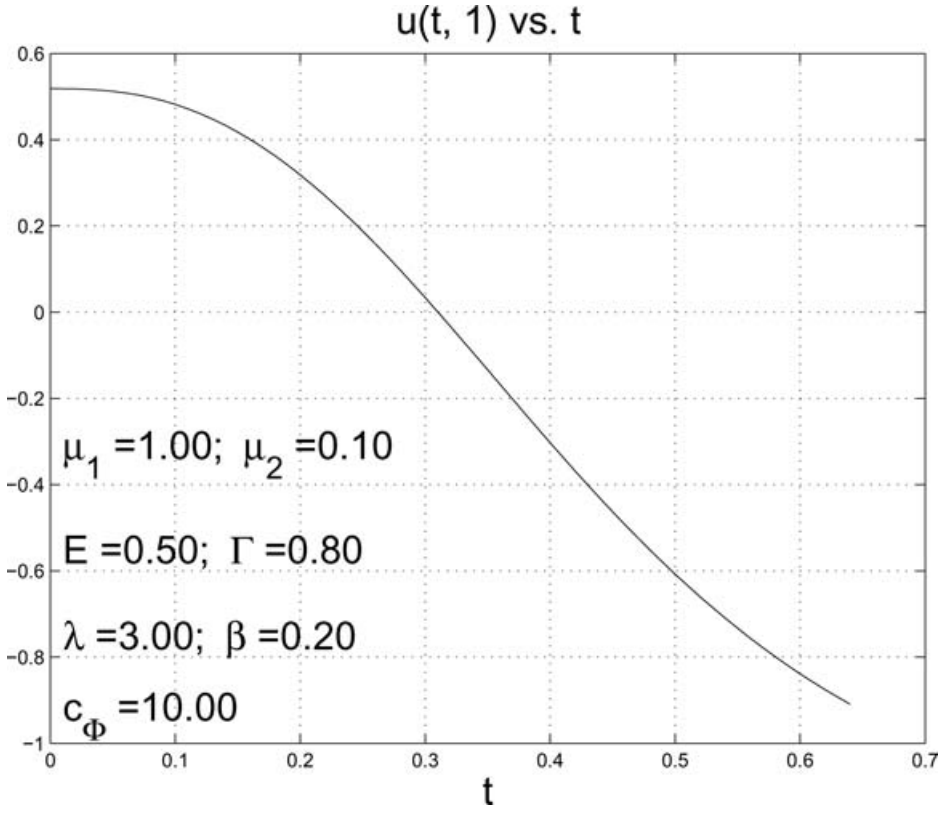

Figure 6. Time evolution of radial displacement at the wound edge during wound closure.

in less than 20 hours for a wound of the size of 0.1 mm $\times$ 0.5 mm inflicted on a wing bud of a 4-day old embryonic chick [2]. For the principal set of parameter values given in Table 3 and with $r_{sp} = 2$ and cell radius $= 0.02$ (both in units of the wound radius), the wound (normalized to unit radius) does close in about one unit of time. This means that time is measured in units of 20 hours. The information may be used as one of the conditions needed to determine the values of parameters in our model not available in the literature and thereby reduce the number of unknown parameters to be measured.

Sensitivity of the solution behavior to values of the epidermal parameters has been investigated by numerical simulations, typically by increasing and decreasing the basic set of parameter values given in Table 1 by 50%. The effects of changing the values of the elastic parameters $\{E, \Gamma, \lambda, \beta\}$ are similar to those in the quasi-static problem. The effects of 50% changes in μ_1 and μ_2 are of the order of 2.5%. The actual data will not be given here because the effects are rather insignificant and, in case of β near β_{cr} not reliable. Further discussion of these effects will await some experimental determination of the

actual parameter values with the capacity for numerical simulations developed herein providing some guide for the design of the relevant experiments.

5. Concluding remarks

In this paper, we have undertaken biodynamical modeling and analysis of embryonic epidermal wound closing for which there does not seem to be any published investigation. In addition to being of independent physiological interest phenomenon, an understanding of epidermal wound repair is expected to contribute to the study of dermal (full-depth) wound healing since wound closure by epidermal migration is known to be one of the three stage of dermal wound closure (occurring between inflammation and extracellular matrix remodeling in scar tissue). Embryonic wound repair has the simplicity of healing without scars and thereby eliminating an additional consideration of the scar formation.

The mathematical model of embryonic epidermal wound healing adopted in this study is founded on the documented observations that actin filaments in cells near the wound edge re-align after wound infliction [5, 6] and that of the wound edge contracts after an actin cable is formed in cells adjacent to the edge [3]. This leaves us with two principal tasks to complete our model formulation: The identification of (1) the biophysical process of cells detecting the presence of a wound for actin re-alignment and (2) the mechanism relating the presence of an action cable and the elastodynamic process of contraction of the wound edge. We dealt with these two tasks through the introduction of (1) the concept of *biosignal asymmetry* and its mathematical representation by a *biosignal asymmetry vector*, and (2) the *active stress postulate* that relates the active stress to the deviation of directional biosignal asymmetry from the mean biosignal asymmetry in Section 3. Together, they provided a reasonable solution to complete the model formulation. Linear elasticity and the Kelvin–Voigt model are adopted for the passive stress measures in the dynamical behavior of epidermal sheet; when and how these should be modified is well understood. Thus, by taking into account the limited experimental information available in the literature, we have succeeded in formulating a physically plausible continuum mechanics model for the study of the biological/physiological phenomenon of embryonic epidermal wound closing.

As with any nonlinear model involving partial differential equations, the time evolution of the displacement field of the epidermis during wound closure requires extensive computations. In our model, these occur in two ways: the determination of the effects of the wound signals on the actin re-alignment and the calculation of the elastodynamic response of the epidermis to the (purse-string) effects of the wound signals. A theory and an associated numerical algorithm have been developed to efficiently compute the effects of wound signals on cells in the epidermis. The importance of the efficiency offered by the algorithm will be even more substantial for noncircular wound

shapes than for the circular wound considered herein. As for computing the elastodynamic response of the epidermis to the purse string contraction effected by the actin cable, we have limited ourselves to the case of a small strain model to investigate the efficacy of the conceptual aspects of the model. The small strain approximations simplify the strain-displacement relations in the elastic and visco-elastic stresses as well as the form of the active stresses in terms of the mean biosignal asymmetry vector. It is understood that small strain approximations would cease to be applicable should the magnitude of strain components become finite or large, particularly at the onset of stress concentration near the end of the wound closing. At that point, model refinement (including the use of a finite strain theory and possibly other modifications) should be undertaken and more appropriate forms of wound signaling and active stress may be adopted without disrupting the conceptual aspects and the general approach of our model.

Numerical results are generated by the model using available parameter values in the literature for the various elastic and visco-elastic moduli and biophysical parameters when they are available. They show that a qualitatively reasonable (time scale for) wound closing behavior by way of the purse-string contraction mechanism is possible provided the range of influence of the biosignal from the cell mass at any location is sufficiently far reaching. This validates a posteriori the elimination of any role of contact signaling in the wound closing process (as it is not realistic to expect that signals received by a cell can be passed on to neighboring cells with no loss of intensity). Sensitivity to model parameter values have been examined. The effects of changes on the elastic parameters are consistent with those in the quasi-static problem. More surprisingly, the solution behavior is rather insensitive to 50% changes to the canonical set of values chosen for the visco-elastic parameters in Table 3. Further insight on the visco-elastic aspects of the solution behavior will await experimental determination of a correct set of parameter values for μ_a, λ, c_m, etc.

To the extent that a circular wound shape is rather special and somewhat artificial, we will not comment further on the solution behavior for this case but be satisfied with the fact that we have developed a physically reasonable model for the embryonic epidermal wound closing phenomenon which actually exhibits wound closure in the actual solution behavior. Model development and numerical simulations for elliptic wound shapes have been reported in [9] and a manuscript on this more general case is being prepared for a near future publication.

Acknowledgment

The research of F.Y.M. Wan was supported by NIH Grants P20-GM066051, NSF SCREMS Grant DMS0112416, and UC Irvine Research Grant 445861. The dissertation of A. Sadovsky was supported in part by a UC Irvine

Mathematics Department Dissertation Fellowship. The authors are appreciative of Professors Qing Nie and James Murray who introduced them to the problem and provided initial guidance to their research. Thanks are also due to P. Martin for his elucidation of wound kinematics, to A. D. Lauder for helpful discussion on cell signaling, and to K. Sadovsky for designing and creating Figure 1.

References

1. J. D. Murray, *Mathematical Biology I: An Introduction*, 3rd ed., New York, Springer-Verlag, Inc., 2002.
2. J. D. Murray, *Mathematical Biology II: Spatial Models and Biomedical Applications*, Springer-Verlag, New York, 2003.
3. S. Nodder and P. Martin, Wound healing in embryos: A review, *Anat. Embryol (Berl)* 195(3):215–228 (1997).
4. J. A. Sherratt, P. Martin, J. D. Murray, and J. Lewis, Mathematical models of wound healing in embryonic and adult epidermis, *IMA J. Math. Appl. Med. & Biol.* 9:177–196 (1992).
5. P. Martin and J. Lewis, The mechanics of embryonic skin wound healing-limb bud lesions in mouse and chick embryos, in *Fetal Wound Healing* (N. S. Adzick and M. T. Longaker, Eds.), pp. 265–279, Elsevier, New York, 1991.
6. P. Martin and J. Lewis, Actin cables and epidermal movement in embryonic wound healing, *Nature* 360:179–183 (1992).
7. J. D. Murray and G. F. Oster, Cell traction models for generating pattern and form in morphogenesis, *J. Math. Biol.* 19:265–279 (1984).
8. J. D. Murray and G. F. Oster, Generation of biological pattern and form, *IMA, J. Math. Appl. in Medic and Biol.* 1:51–75 (1984).
9. A. Sadovsky, *A Biodynamical Study of Epidermal Wound Repair in Embryos*, Ph.D. thesis, University of California, Irvine, 2004.
10. J. A. Sherratt, A perturbation problem arising from a mechanical model for epithelial morphogenesis, *IMA J. Appl. Math.* 47(2):147–162 (1991).
11. J. A. Sherratt, Actin aggregation and embryonic epidermal wound healing, *J. Math. Biol.* 31:703–716 (1993).
12. A. Sadovsky and F. Y. M. Wan, *The Closing of an Elliptical Wound*, to be submitted for publication, 2007.
13. Y. C. Fung, *Foundations of Solid Mechanics*, Englewood Cliffs, JN, Prentice Hall, 1965.
14. G. J. Hergott, M. Sandig, and V. I. Kalnins, Cytoskeletal organisation of migrating retinal pigment epithelial cells during wound healing in organ culture, *Cell Motil.* 13:83–93 (1989).
15. J. A. Sherratt, *Mathematical Model of Wound Healing*, Ph.D. thesis, University of Oxford, 1991.
16. J. A. Sherratt and J. D. Murray, Models of epidermal wound healing, *Proc. R. Soc. Lond. B*, 241:29–36 (1990).
17. M. Abramowitz and I. Stegun, *Handbook of Mathematical Functions, with Formulas, Graphs, and Mathematical Tables*, New York, Dover Publ., 1965.

18. B. HINZ and G. GABBIANI, Mechanisms of force generation and transmission by myofibroblasts, *Curr Opin Biotechnol.* 14(5):538–546 (2003).

19. S. RAMTANI, E. FERNANDES-MORIN, and D. GEIGER, Remodeled-matrix contraction by fibroblasts: Numerical investigations, *Comp. in Biology and Medicine*, 32:283–296 (2002).

20. B. ALBERTS, ET AL., *Essential Cell Biology: An Introduction to the Molecular Biology of the Cell*, 2nd ed., New York: Garland Publ., 1998.

21. D. J. TSCHUMPERLIN, G. DAI, G. I. V. MALY, T. KIKUCHI, L. H. LAIHO, A. K. MCVITTIE, K. J. HALEY, C. M. LILLY, P. T. C. SO, D. A. LAUFFENBURGER, R. D. KAMM, and J. M. DRAZEN, Mechanotransduction through growth-factor shedding into the extracellular space, *Nature* 429:83–86 (2004).

UNIVERSITY OF CALIFORNIA

(Received September 8, 2006)